Morphology and Mechanical Properties of Styrene–Ethylene/Butylene–Styrene Triblock Copolymer/High-Density Polyethylene Composites

Xiju Yu, Zhen Zheng, Jiaming Lu, Xinling Wang

School of Chemistry and Chemical Technology, Shanghai Jiao Tong University, Shanghai 200240, People's Republic of China

Received 4 February 2007; accepted 21 May 2007
DOI 10.1002/app.26967
Published online 25 September 2007 in Wiley InterScience (www.interscience.wiley.com).

ABSTRACT: The morphology and mechanical properties of a styrene–ethylene/butylene–styrene triblock copolymer (SEBS) incorporated with high-density polyethylene (HDPE) particles were investigated. The impact strength and tensile strength of the SEBS matrix obviously increased after the incorporation of the HDPE particles. The microstructure of the SEBS/HDPE blends was observed with scanning electron microscopy and polar optical microscopy, which illustrated that the SEBS/HDPE blends were phase-separation systems. Dynamic mechanical thermal analysis was also employed to characterize the interaction between SEBS and HDPE. The relationship between the morphology and mechanical properties of the SEBS/HDPE blends was discussed, and the toughening mechanism of rigid organic particles was employed to explain the improvement in the mechanical properties of the SEBS/HDPE blends. © 2007 Wiley Periodicals, Inc. J Appl Polym Sci 107: 726–731, 2008

Key words: elastomers; mechanical properties; morphology; polyethylene (PE); structure-property relations

INTRODUCTION

The styrene–ethylene/butylene–styrene triblock copolymer (SEBS), which is synthesized through the selective hydrogenation of styrene–butadiene–styrene, has attracted a great deal of interest in academia and commercial fields. It has many outstanding properties, such as good stability, good heating resistance, and resistance to oxidation, ozone, and ultraviolet radiation. It is always used as an interfacial modifier in polymer blends to improve the miscibility of two matrix components.[1–4] However, SEBS also acts as a polymer matrix in high-performance, fiber-reinforced polymer composites, which are usually used in aerospace and military applications. However, the impact strength of SEBS is not so good when it is used as a polymer matrix. One of the tendencies is to improve the impact energy of SEBS without a reduction of the viscosity.

There has been much research focused on the improvement of the impact strength of polymer materials over the past several decades.[5–8] Rubber-toughened plastics have been widely used to improve the impact properties of commercial materials. For those polymer matrices, there is a two-phase system in which rubber particles are dispersed in a polymer matrix and the dispersed particles act as stress concentrators and inducers of energy dissipation by both crazing and shear yielding of the composites. However, toughness enhancement through the addition of relatively high amounts of low-modulus polymers usually leads to a marked reduction of other properties, such as the strength and stiffness.[9] To solve these problems, a rigid-organic-filler-toughening method, developed first by Kurauchi and Ohta,[10] has been introduced. According to an investigation of the blending of polycarbonate with acrylonitrile-butadiene-styrene (ABS) or styrene-acrylonitrile (SAN) systems, rigid organic particles (nonelastomer particles) can improve the toughness of polymer materials, and the toughening mechanism has been explained as follows: the impact energy is absorbed by large plastic deformation of brittle particles dispersed in a ductile matrix. This concept is called cold drawing. Then, Inoue and coworkers[11,12] further investigated these toughening systems, pointing out the conceivable requirements for the development of toughening in ductile/brittle systems, for which interfacial action is better between ductile and brittle phases.

The incorporation of high-density polyethylene (HDPE) into SEBS is expected to ameliorate the problems, and a good interaction between the HDPE and SEBS phases is also expected to be obtained because the hydrogenated ethylene–butadiene blocks in SEBS triblock copolymers are soluble with HDPE macromolecules.[13,14] The objective of this study was

Correspondence to: Z. Zheng (zzheng@sjtu.edu.cn).

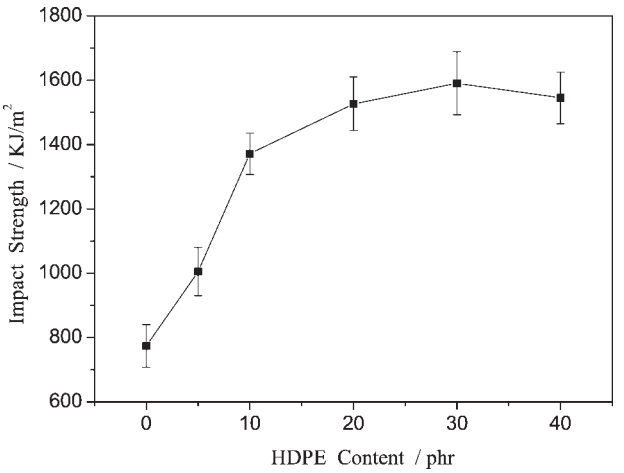

Figure 1 Variation of the Charpy impact strength with the HDPE content in the SEBS/HDPE blends.

to examine the impact strength, tensile properties, and two-phase morphology of binary SEBS/HDPE blends to determine the correlation between the morphology and mechanical properties and demonstrate a new method for improving the impact strength of SEBS without the reduction of other mechanical strengths.

EXPERIMENTAL

Materials

All the raw materials used in this study were commercial polymers. The SEBS triblock copolymer (Kraton G1652, Shell Chemical Co., Shanghai, China) had molecular weights for the polystyrene (PS) block and ethylene/butylene (E/B) block of 7500 and 37,500, respectively, and the PS weight fraction was 28.6%. HDPE [M80064; melt flow index = 8.0 g/10 min (ASTM D 1238)] was supplied by Saudi Basic Industries Corp. (Riyadh, Saudi Arabia).

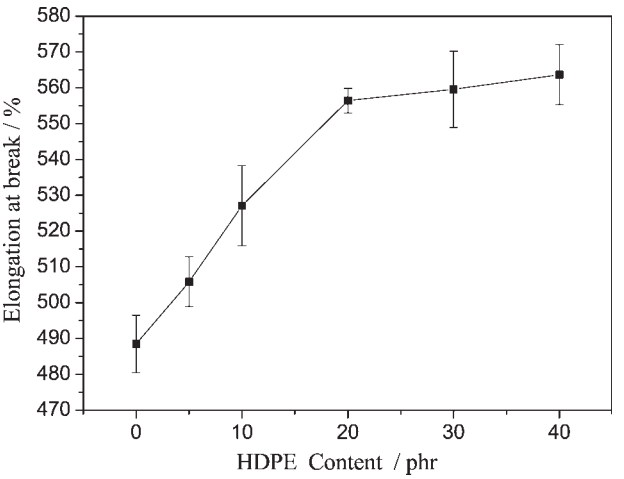

Figure 2 Elongation at break versus the HDPE content in the SEBS/HDPE blends.

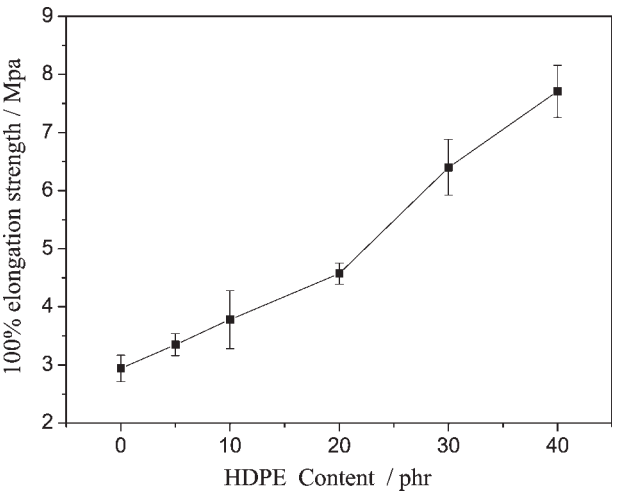

Figure 3 Elongation strength (100%) versus the HDPE content in the SEBS/HDPE blends.

Preparation of the samples

All the materials were dried separately in an oven to remove water before their use. SEBS and HDPE were blended simultaneously for 25 min in a torque rheometer (XSS-300, Kechuang Machinery Co., Shanghai, China). During this process, the speed of the rotator was 60 rpm/min, and the temperature was 180°C. After the blending, the appropriate specimens were treated on a plate vulcanization molding machine (Zhejiang Huzhou Hongtu Machinery Co., Ltd., Huzhou, Zhejiang Province, China) according to the following steps:

1. Preheating without pressure at room temperature for 20 min and deflation for 2 min.
2. Compression under a pressure of 10 MPa at 150°C for 10 min.
3. Cooling to room temperature under a pressure of 5 MPa for 15 min.

Finally, the samples were cut to a standard size for subsequent measurements.

Measurement of the samples

Notched Charpy impact testing was carried out according to GB 13525-92 with a testing machine (Impact Test Equipment, Ray-Ran Test Equipment Ltd., Nuneaton, United Kingdom); the free sample length was 110 mm, the width was about 10 mm, and the thickness was about 1 mm.

Tensile testing were performed according to GB 528-92 on an Instron 4465 universal testing machine (Instron Corp., Canton, MA); the free sample was dumbbell-shaped, and the thickness was about 2 mm. A field emission scanning electron microscope (model JSM-7401F, JEOL Ltd., Tokyo, Japan) was used to observe the microstructures of the compo-

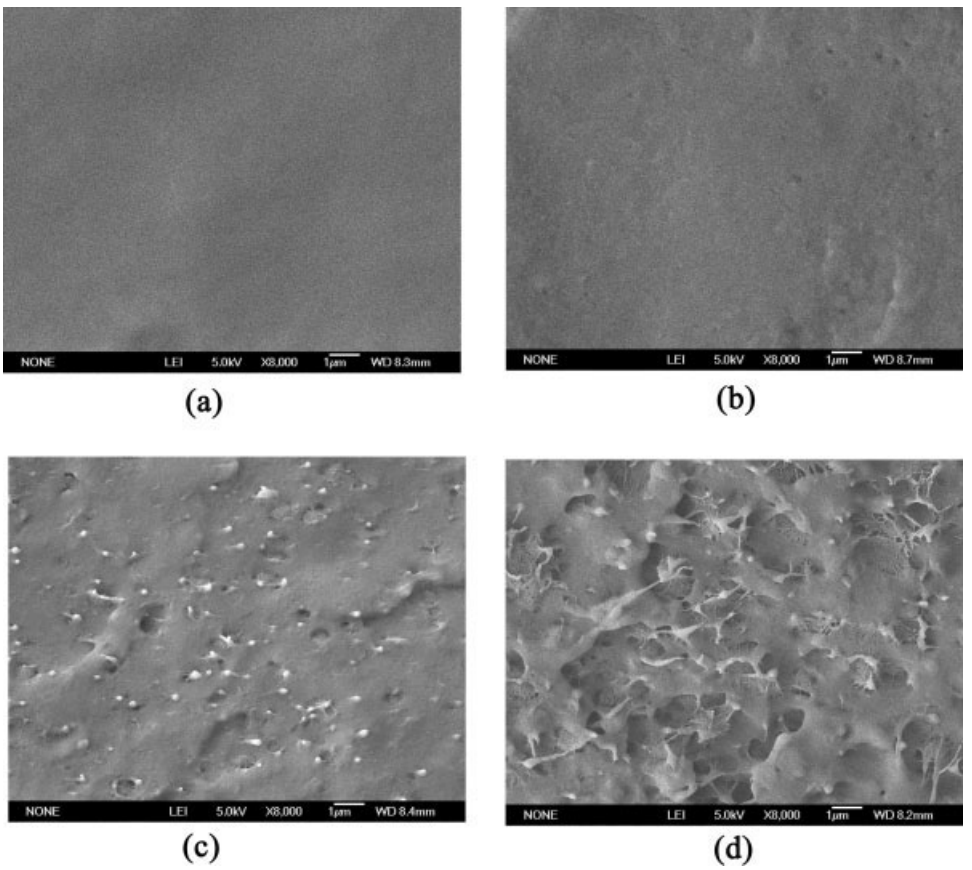

Figure 4 Scanning electron microscopy photographs of fracture surfaces with different HDPE contents in the SEBS matrix: (a) 0, (b) 5, (c) 20, and (d) 40 phr.

sites. All the specimens were fractured in liquid nitrogen and gold-sputtered before observation.

The morphology of the samples was also observed with a polar optical microscope (Leica DM LP, Leica Microsystems GmbH, Wetzlar, Germany). All the specimens were compressed into films by hot compression before observation.

The crystalline structure of HDPE/SEBS was obtained by X-ray diffraction (Rigaku International Corp., Tokyo, Japan). The experiment was performed with a Rigaku DmaxRC diffractometer with a Cu target and a rotating-anode generator operated at 40 kV and 100 mA. The scanning rate was 4°/min from 10 to 40°. The film sample for X-ray diffraction measurements was prepared by compression molding at 150°C and 10 MPa. The transmission electron micrographs were taken from 80–100-nm-thick microtomed sections with a transmission electron microscope with a 100-kV accelerating voltage.

Dynamic mechanical tests were operated on a TA Q800 dynamic mechanical analyzer (TA Instruments, Inc., New Castle, DE) in a tensile mode. Temperature scans were conducted at a heating rate of 3°C/min with a fixed measurement frequency of 1 Hz, ranging from −130 to 150°C. The free sample length was 50 mm, the width was about 5 mm, and the thickness was about 2 mm.

RESULTS AND DISCUSSION

Impact behavior and tensile properties

At present, there are many studies about the modification of SEBS elastomer systems with additives; the mechanical properties, thermal properties, and rheological properties are improved through blending with additives such as resins, stuffing, and oil.

Resin modifications are widely used because of the universality of the materials and the distinct results. As for HDPE, after the addition of HDPE, many capability indices are better than those of many other resins. However, research has been limited to the relationship between the component changes and properties. This study was set up to determine the relationship between the compositions, morphology, and use efficiency. Accordingly, the design of specific materials could be supervised and achieved.

Figure 1 depicts the variation in the notched Charpy impact strength of the SEBS/HDPE compo-

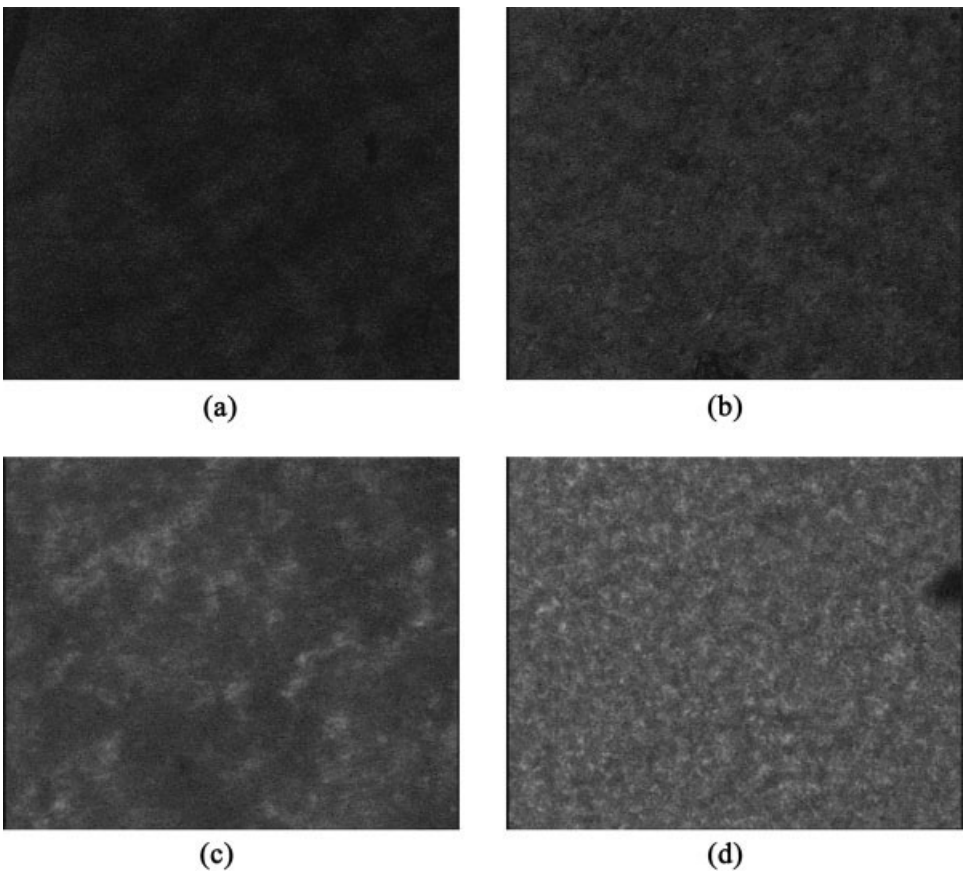

Figure 5 Polar optical microscopy images for SEBS/HDPE blends with different HDPE contents: (a) 100/0, (b) 100/10, (c) 100/30, and (d) 0/100 SEBS/HDPE.

sites with the HDPE content. The impact energy first increased with an increase in the HDPE content and then remained steady when the HDPE content was greater than about 20 phr. This phenomenon was in accordance with the results of nonelastomer toughening.[10] For rigid-organic-filler-toughening composites, the impact strength can be improved only with a certain variation of the organic particles, and once the content of the particles is beyond a certain limit, there will be no improvement and even a slight decrease. That is different from rubber-toughening composites, in that the impact strength of the latter blends always increases with an increase in the rubber content.

In Figures 2 and 3, the increasing tendency of the elongation at break and 100% elongation strength is similar to that of the impact properties. The addition of HDPE significantly enhances the elongation at break of the composites, and this is supposed to the reason that it strengthens the cohesive force between the HDPE phase and SEBS phase.[15,16]

The high energy absorption capability of SEBS/HDPE blends can be attributed partly to the ductility of the HDPE particles. Thus, the total energy absorbed in the fracture process of polymer materials is the summation of the energy absorbed by crazing, the shear yielding band, and the deformation of dispersed phase particles. In Kuracuchi and Ohta's study,[10] only the energy absorbed through cold-drawing deformation of the rigid dispersed phase was noticed, and the energy absorbed by crazing and the shear-yielding band of the matrix was neglected.

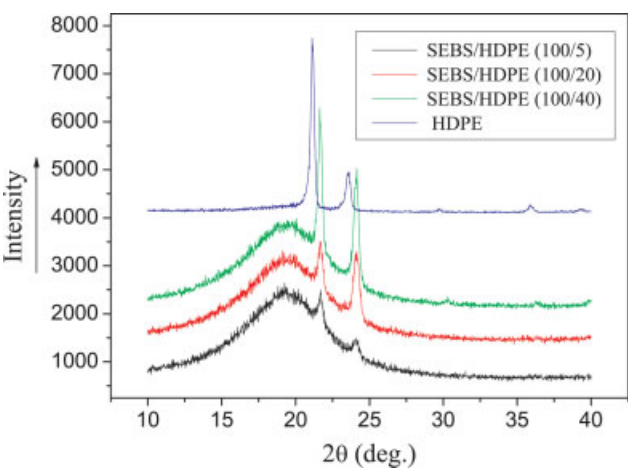

Figure 6 X-ray diffraction patterns for SEBS and SEBS/HDPE blends. [Color figure can be viewed in the online issue, which is available at www.interscience.wiley.com.]

TABLE I
Analysis of the XRD Patterns of the HDPE Particles and HDPE/SEBS Blends

Sample	2θ (°)	Length (nm)	2θ (°)	Length (nm)
HDPE	21.154	0.750	23.575	0.681
SEBS/HDPE (100/40 w/w)	21.665	0.567	24.114	0.554

Meanwhile, the ductility of SEBS materials has also contributed to the improvement of the impact energy. For this reason, when the matrix is brittle, it is difficult to deform it and produce the hydraulic pressure that will constrain the rigid disperse phase to brittlely deform before polymer fracture; hence, the impact strength of a polymer blend cannot be improved effectively with rigid particles. When the matrix contains some ductility, hydraulic pressure can be produced easily, and the polymer systems can be toughened.[17]

Morphology of the SEBS/HDPE blends

The fundamental morphology of neat SEBS is a particular microphase-separation structure due to the incompatibility between the different connected block chains.[18] Figure 4 presents the microstructures of fracture surfaces of SEBS/HDPE blends, exhibiting the expected two-phase morphology that has been found in other insoluble blends.[19] Four compositions are shown in Figure 4, and the concentrations of HDPE in the SEBS matrix were 0, 5, 30, and 40 phr, respectively. At a low HDPE concentration, there was no clear observation of a double-phase structure because of the partial compatibility between SEBS and HDPE. With an increasing HDPE concentration, the microstructure of the SEBS/HDPE blends produced an insoluble polymer blend structure, as shown in Figure 4(c,d).

Polar optical microscopy graphs were employed to detect the morphology of the SEBS/HDPE blends, as shown in Figure 5. There are four compositions shown: pure SEBS, 10 or 30 phr HDPE in the SEBS matrix, and pure HDPE. From the graph, we know that the change in SEBS had an influence on the crystal of HDPE. Although HDPE was partly soluble in SEBS as mentioned before, the HDPE crystal is clearly shown, and the phase-separation structure can be found.

The X-ray diffraction spectra of HDPE and HDPE/SEBS are shown in Figure 6. The HDPE and SEBS/HDPE crystals obtained in this study were obviously in the form. As shown in Figure 6, the diffraction patterns of the composites of SEBS/HDPE with HDPE concentrations ranging from 5 to 40 phr were similar to one another. The peak position shifted to a slightly large angle (Table I). To estimate the crystallite size from the broadening of the diffraction pattern, a method based on the Scherrer equation is generally used. The crystallite dimension, or coherence length, perpendicular to the (*hkl*) plane (L_{hkl}) can be calculated with the Scherrer equation:[20]

$$L_{hkl} = \frac{K\lambda}{\beta_{hkl} \cos \theta_{hkl}} \quad (1)$$

where K is the Scherrer constant (0.9 here), λ is the wavelength of the X-rays, θ_{hkl} is the Bragg angle, and β_{hkl} is the diffraction half-width.

Obviously, the crystallite dimensions of HDPE in the SEBS/HDPE systems were smaller than those of pure HDPE. The crystallite dimensions of a semicrystalline polymer are functions of the crystallization temperature and the density of nucleation. The smaller crystallite size seemed to suggest that nuclei existed in the processing of crystallization.[21] Therefore, SEBS had a nucleating effect on the crystallization of HDPE. However, for various concentrations of HDPE in HDPE/SEBS, there was no clear change in the crystallite.

Dynamic mechanical thermal analysis

The pure SEBS specimen showed two peak loss tangents. One was the glass transition for E/B (the low-temperature peak); the other was for the PS block (the high-temperature peak). As shown in Figure 7, the intensity of the loss tangents of the PS block decreased and even disappeared as the amount of HDPE increased, especially above 10 phr. On the contrary, the intensity of the soft-phase E/B blocks increased with increasing HDPE concentration. The reason is that the molecular chains of HDPE and SEBS responded to the change in the loss tangent. The intensity of the low-temperature peak could be attributed to the entwisting of the E/B block of SEBS and HDPE chains, which made the E/B chain move with

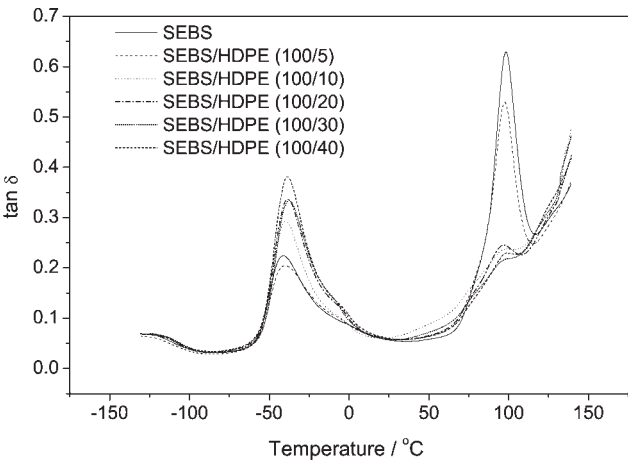

Figure 7 Dynamic loss tangent (tan δ) values of SEBS/HDPE blends with different HDPE contents.

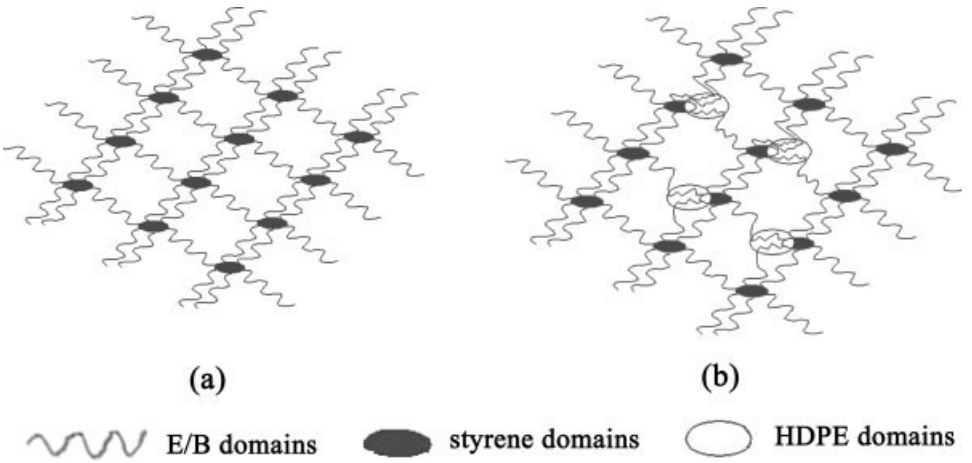

Figure 8 Schematic diagrams of SEBS and SEBS/HDPE blends: (a) SEBS and (b) some droplets of HDPE dispersed in bulk SEBS.

more difficulty. The PS block was dissolved by the HDPE chains, and this made it move more easily.

Figure 8(a) shows a schematic diagram of SEBS microstructures; the dark cylinders represent styrene domains, and the springs represent the elastic and flexible E/B domains; while mixing with the HDPE phase, as shown in Figure 7(b), the E/B domains near the HDPE interface suggest good interactions of these segments.

CONCLUSIONS

The incorporation of HDPE particles into SEBS resins can improve the notched impact strength and elongation at break of the composites. The toughening mechanism is correlated to rigid organic filler toughening elastomers; this is also called cold drawing and can be explained as positive actions of nonelastomer toughening. Under the inducement of compressive stress, HDPE particles produce larger plastic deformation and absorb more impact energy. On the other hand, HDPE molecular chains have an affinity to E/B blocks because of their similar natures, but they produce solubility problems with the styrene block of SEBS because of the polarity difference. That is the reason for the partial phase separation in SEBS/HDPE composites. When the concentration of HDPE is very low, the interfacial action is good, and phase separation hardly appears. When the concentration of HDPE is more than 10 phr, the phase-separation phenomenon begins to appear partly, and this leads to the poor interfacial action. The detected morphology of the SEBS/HDPE systems has a typical double-phase microstructure. Both scanning electron microscopy and polar optical microscopy show that with an increasing concentration of HDPE, the microstructure of SEBS/HDPE blends produces a two-phase structure, the decentralization of HDPE becomes quite uniform, and the effect of toughening is better. HDPE has been found to be a suitable original particle for toughening SEBS.

The authors thank the Quartermaster Institute of the General Logistic Department of the Chinese People's Liberation Army and Hunan Sino-Thai Special Arming Co., Ltd., of Hunan Province for their sustainable support of our research.

References

1. Chirawithayaboon, A.; Kiatkamjornwong, S. J Appl Polym Sci 2004, 91, 742.
2. Hisamatsu, T.; Nakano, S.; Adachi, T.; Ishikawa, M.; Iwakura, K. Polymer 2000, 41, 4803.
3. Raha, S.; Kao, N.; Bhattacharya, S. N. Polym Eng Sci 2005, 45, 1432.
4. Li, Y. L.; Xie, T. X.; Yang, G. S. J Appl Polym Sci 2005, 95, 1354.
5. Bai, H.; Zhang, Y.; Zhang, X.; Zhou, W. J Appl Polym Sci 2006, 101, 54.
6. Yang, L.; Hu, Y.; Guo, H.; Song, L.; Chen, Z.; Fan, W. J Appl Polym Sci 2006, 102, 2560.
7. Canto, L. B.; Hage, E.; Pessan, L. A. J Appl Polym Sci 2006, 102, 5795.
8. Tjong, S. C.; Bao, S. P.; Hang, G. D. J Polym Sci Part B: Polym Phys 2005, 43, 3112.
9. Perkins, W. G. Polym Eng Sci 1999, 39, 2445.
10. Kurauchi, T.; Ohta, T. J Mater Sci 1983, 19, 1699.
11. Angola, J. C.; Fujita, Y.; Sakai, T.; Inoue, T. J Polym Sci Part B: Polym Phys 1988, 26, 807.
12. Koo, K. K.; Inoue, T.; Miyasaka, K. Polym Eng Sci 1985, 25, 741.
13. Li, J.; Favis, B. D. Polymer 2001, 42, 5047.
14. Kim, T. Y.; Kim, D. M.; Kim, W. J.; Lee, T. H.; Suh, K. S. J Polym Sci Part B: Polym Phys 2004, 42, 2813.
15. Bureau, M. N.; Kali, H. El; Denault, J.; Dickson, J. I. Polym Eng Sci 1997, 37, 377.
16. Tjong, S. C.; Xu, S. A. J Appl Polym Sci 1998, 68, 1099.
17. Peng, J.; Wei, G. S.; Zhang, Y. D. J Appl Polym Sci 2003, 88, 2478.
18. Wang, Y.; Shen, J. S.; Long, C. F. Polymer 2001, 42, 8443.
19. Mironi-Harpaz, I.; Narkis, M. J Appl Polym Sci 2001, 81, 104.
20. Kakudo, M.; Kasai, N. J Polym Sci Polym Lett Ed 1972, 10, 424.
21. Wu, D.; Zhou, C.; Fan, X.; Mao, D.; Bian, Z. Polym Polym Compos 2005, 13, 61.